ISSN 0029-3865

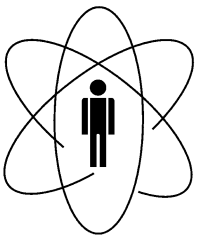

CBPF - CENTRO BRASILEIRO DE PESQUISAS FÍSICAS

Rio de Janeiro

Notas de Física

CBPF-NF-003/18

March 2018

A calculation model to half-life estimate of two-proton radioactive decay process

O.A.P Tavares and E.L. Medeiros

MINISTÉRIO DA CIÊNCIA, TECNOLOGIA, INOVAÇÕES E COMUNICAÇÕES

A calculation model to half-life estimate of two-proton radioactive decay process[1,2]

O A P Tavares and E L Medeiros[3]

Centro Brasileiro de Pesquisas Físicas - CBPF/MCTIC
Rua Dr. Xavier Sigaud 150, 22290-180 Rio de Janeiro-RJ, Brazil

Abstract - Partial half-life of the radioactive decay by the two-proton emission mode has been estimated for proton-rich nuclei of mass number $18 < A < 68$ by a model based on the quantum mechanical tunneling mechanism through a potential barrier. The Coulomb, centrifugal and overlapping contributions to the barrier have been considered within the spherical nucleus approximation. The present calculation method has shown adequate in reproducing the existing experimental half-life data for ^{19}Mg, ^{45}Fe, ^{48}Ni, and ^{54}Zn 2p-emitter nuclides within a factor six. For ^{67}Kr parent nucleus the calculated partial 2p-decay half-life has been found ten times greater than the recent, unique measured value at RIKEN Nishina Center. Prediction for new, yet unmeasured cases of two-proton radioactivity are also reported.

[1]In celebration of the 70th anniversary of the detection of π-mesons produced in the laboratory.

[2]Accepted for publication in The European Physical Journal A on March 15, 2018.

[3]Corresponding author. E-mail: emil@cbpf.br

1 Introduction

Since the discovery of the radioactivity by Becquerel a hundred and twenty-one years ago [1], different modes of nuclear decays have been identified up to recent years: alpha-, beta-, and neutron-decay, spontaneous fission, emission of neutron, proton, and alpha-particle accompanying β^--decay, cluster radioactivity (spontaneous emission of ^{14}C, ^{20}O, $^{24–26}$Ne, ^{28}Mg, and ^{34}Si from heavy nuclei), delayed particle emission following β^+ or electron capture, and cold fission as well. In the last two decades or so, attention has been paid to the new modes of radioactive decay that occur when reaching the limits of nuclear stability, *i.e.*, the vicinity of neutron and proton drip lines and beyond. A number of nuclides at these extreme mass regions do exhibit β-decay into excited levels of the product nuclei which, therefore, can emit one or more nucleons. Besides, in some cases the Q-value for the emission of one or two nucleons becomes positive, and thus they can be emitted from the ground-state of a parent nucleus. In this context, two-proton radioactivity appears as a rare nuclear decay process, perhaps the most complex one, that has been observed in proton-rich, less-massive nuclei of $A < 68$ located near the proton drip line.

The possibility of the two-proton radioactivity was pointed out for the first time by Zeldovich [2] and, at the same time, the description of the process was given by Goldansky [3]. The prediction of two-proton emission from neutron-deficient nuclei had its first confirmation with the experimental observation of $^{45}\mathrm{Fe} \rightarrow {}^{43}\mathrm{Cr} + \mathrm{p} + \mathrm{p}$ decay by Pfützner *et al.* [4] at GSI (Germany) and, independently, by Gioninazzo *et al.* [5] at GANIL (France). These research groups obtained a half-life in the range $\sim$ 3–8 ms for the 2p-decay process in ^{45}Fe. Since then a number of experiments on correlated two-proton emission have been conducted, five cases are perfectly identified presently, and their experimental half-lives well determined within the difficulties the extremely low decay rates impose (see Table 1). The last, most recent, 2p-decay case investigated concerns the discovery of correlated two-proton emission from ^{67}Kr parent nucleus at the RIKEN Nishina Center [27], where the research group obtained 20 ± 8 ms for the half-life of this newly case of 2p-decay. Recent experiments of the last six years or so have confirmed the 2p radioactivity in ^{45}Fe [16] and ^{54}Zn [26] at GANIL (France), and ^{19}Mg [12] at Michigan-NSCL (USA). Also at Michigan-NSCL it was detected for the first time the 2p radioactivity of ^{48}Ni [22–24].

Soon after the pioneering work of Goldansky [3] a number of theoretical approaches to describe the two-proton radioactivity were published (see, for instance, [30–33]). Here, we highlight the works by Grigorenko *et al.* who have investigated the two-proton radioactivity in the framework of their three-body model [34, 35]. Among other topics, they studied the dependence of half-life

upon the decay energy for ^{54}Zn, ^{58}Ge, ^{62}Se, and ^{66}Kr 2p-emitter nuclides and compared results to the quasiclassical estimates. Predictions of true 2p-decay half-life were obtained for nuclei of $Z < 40$ along the proton drip line, with indication for ^{30}Ar, ^{58}Ge, ^{62}Se, and ^{66}Kr as new candidate nuclides for pioneering experimental investigation on correlation of the decay products [35].

It is worthwhile to mention the complete review article on decay modes of nuclei close to the limits of stability that has been presented by Pfützner *et al.* [36] who have also included the current theoretical aspects and description of the complex, rare process of 2p-decay.

More recently, Olsen *et al.* [37] have used the nuclear density functional theory (DFT) to investigate the 2p radioactivity and find new 2p-emitter nuclides heavier than strontium. Competition between 2p-decay and α-decay has been predicted to some cases with a chance of being observed (nuclei around ^{103}Te–^{110}Ba). In addition, the authors conclude that there are at present only two regions of candidate nuclides for which true 2p-decay can be observed: germanium to krypton and just above tin.

It is also important to mention the description of the simple formalism to two-proton emission developed by Delion *et al.* [38], where it is assumed that the two protons are emitted from a correlated pairing state. Their approach demonstrates the existence of a strong dependence of the half-life upon the proton-proton coupling strength.

Finally, a few months ago, the effective liquid drop model in the spherical approximation for the atomic nuclei has been used by Gonçalves *et al.* [39] to estimate the half-lives of two-proton radioactivity of a number of emitter nuclides of mass number $A < 70$. Such a model has shown good agreement with the existing data for ^{19}Mg, ^{45}Fe, ^{48}Ni, and ^{54}Zn parent nuclei, and it points to new promising cases to be measured as well.

Some years ago we were successful in developing a semiempirical, one-parameter model to systematize the α-decay half-life data of bismuth isotopes [40]. This calculation model was constructed on the basis of a quantum-mechanical tunneling mechanism through a Coulomb-plus-centrifugal-plus-overlapping potential barrier within the spherical nucleus approximation. This routine calculation proved again very adequate in systematizing not only a large number of α-decay cases [41–43], but, subsequently, the half-life data of all cases of one-proton radioactivity [44] as well as the cases for spontaneous emission of heavy clusters from trans-lead nuclei (known as exotic radioactivity) [45, 46]. So, we thought it worthwhile to apply our original model description to obtain half-life estimates of two-proton radioactivity cases.

The good agreement achieved between calculated and measured half-life data in the cases

for alpha, one-proton, and cluster radioactivity mentioned above has stimulated us to extend our quantum-mechanical tunneling approach to obtain half-life estimates for the five known 2p-decay cases, as well as to make half-life predictions for new, yet unmeasured radioactive 2p-decay cases.

In the present paper we have tried to obtain an estimate of the half-life of the two-proton radioactive process by an unusual formalism, quite different from those currently used in describing this process as a three-body problem [35, 36]. Thus, the present study has been undertaken with the intention of developing an alternative, practical calculation method to obtain half-life values of the 2p radioactive process, not to describe the details of the physical process itself.

After introducing the bases of the proposed model we will describe here to some detail the routine calculation, present the calculated half-life values, compare them with the measured ones, and give estimates for new 2p-decay cases. We anticipate that in the present analysis on two-proton radioactivity a quite good agreement has been also achieved between each other data.

2 Calculation model for 2p-decay half-life

It is considered here the pure nuclear two-proton decay process, *i.e.*, the so-called true 2p-decay, in which process the separation energy of two protons of a parent nucleus $(Z_{\rm P}, A_{\rm P})$ is negative, thus making it possible the formation of the daughter nucleus $(Z_{\rm D} = Z_{\rm P} - 2, A_{\rm D} = A_{\rm P} - 2)$ by the emission of two protons. True two-proton emission from proton-rich nuclei in the vicinity of the proton-drip line cannot be treated as a sequential emission of two protons for the daughter nucleus after the eventual emission of the first proton may have a negative $Q_{\rm p}$-value, thus making prohibitive the emission of the second proton. (Of course, if the $Q_{\rm p}$-value for both parent and daughter nuclei were positive quantities this mechanism would be a sequential two-proton emission.) In addition, since ^{2}He is an unbound system, it would be very unlikely that two protons could be emitted together as forming a 2p-cluster. Therefore, two-proton radioactivity should be more generally described by a *simultaneous* emission of two protons, but escaping from the nucleus *separately*.

2.1 Energy available in the 2p-decay process

Since the transmutation $(Z_{\rm P}, A_{\rm P}) \rightarrow (Z_{\rm D}, A_{\rm D}) + {\rm p}_1 + {\rm p}_2$ is strictly a nuclear process, the chief quantity $Q_{\rm 2p}$-value is evaluated by the current mass-energy balance, but from the nuclear (rather

than atomic) mass-values, $m_{\rm i}$ (i = P, D, p), *i.e.*,

$$Q_{\rm 2p} = [m_{\rm P} - (m_{\rm D} + 2m_{\rm p})] \cdot F \quad \text{MeV} \tag{1}$$

in which $F = 931.4940038$ MeV/u. The m's are obtained by the usual way, namely,

$$m = A - Zm_{\rm e} + \left(\Delta M + kZ^{\beta}\right), \tag{2}$$

where $m_{\rm e} = 0.54857990 \times 10^{-3}$ u is the electron rest mass, and ΔM is the atomic mass-excess, the values of which (expressed in MeV) are here those from the AME 2016 (the most recent atomic mass evaluation) by Wang *et al.* [28]. The quantity kZ^{β} represents the total binding energy of the Z electrons in the atom, where the constants k and β take the values

$$\begin{aligned} k &= 13.6 \times 10^{-6} \text{ MeV}, \quad \beta = 2.408 \quad \text{for } Z < 60 \\ k &= 8.7 \times 10^{-6} \text{ MeV}, \quad \beta = 2.517 \quad \text{for } Z \geq 60 \end{aligned} \tag{3}$$

as they come from data reported by Huang *et al.* [47].

By combining equations (1)–(3) gives

$$Q_{\rm 2p} = \Delta M_{\rm P} - \Delta M_{\rm D} - 2\Delta M_{\rm H} + k\left[Z_{\rm P}^{\beta} - Z_{\rm D}^{\beta} - 2\right] \text{ MeV}, \tag{4}$$

where the last term represents the effect of the screening to the nucleus caused by the surrounding electrons. For parent nuclei of $Z < 60$ (like the ones listed in Table 1) equation (4) reduces to

$$Q_{\rm 2p} = \Delta M_{\rm P} - \Delta M_{\rm D} + 13.6 \times 10^{-6}\left(Z_{\rm P}^{2.408} - Z_{\rm D}^{2.408}\right) - 14.57796842 \quad \text{MeV}. \tag{5}$$

The uncertainty in $Q_{\rm 2p}$-value, $\delta Q_{\rm 2p}$, comes essentially from the uncertainties $\delta\Delta M$ associated with the ΔM's of the parent and daughter nuclei, and their values are those reported in the AME2016 tables [28].

2.2 Basic assumptions of a simple, true 2p-decay model

Twelve years ago, we developed a simple, one-parameter, semiempirical model based on the current quantum mechanical tunneling mechanism through a potential barrier to evaluate the decay rate of bismuth isotopes [40]. The successful application of such a calculation method to all existing alpha-emitter nuclides [41–43], one-proton radioactive decay cases [44], and also to all known cases

of heavy clusters emission from nuclei (the so-called exotic decays [45, 46]) led us to extend our half-life calculation model to cases of radioactive decay by the emission of correlated two protons that have been observed from 2000 on in some proton-rich nuclei of $A > 18$ located near the proton drip line (Table 1). Here, it is supposed that the emission of two protons in a ground-state to ground-state transition takes place on the grounds of the following assumptions:

i) the two protons are thought to be emitted simultaneously, but in a separate way, forming two virtual, intermediate, daughter nuclei ($Z_{\rm V} = Z_{\rm P} - 1, A_{\rm V} = A_{\rm P} - 1$) as shown schematically in figure 1;

ii) the total energy available in the 2p-decay process as given by equation (5) is shared between the two virtual, intermediate 1p emission processes in such a way that

$$Q_{\rm p_1} = \epsilon Q_{\rm 2p}\,, \quad Q_{\rm p_2} = (1-\epsilon)Q_{\rm 2p}\,, \tag{6}$$

where parameter ϵ varies continuously in the interval $[0, 1]$ (figure 1);

iii) the frequency of assaults of each proton to the potential barrier is calculated as usually, *i.e.*,

$$\lambda_{0_1} = K\sqrt{\epsilon}\,, \quad \lambda_{0_2} = K\sqrt{1-\epsilon}\,, \quad K = \frac{\sqrt{2}}{2a}\sqrt{\frac{Q_{\rm 2p}}{\mu_{0\rm V}}}\,, \tag{7}$$

and the total number of assaults to the barrier per unit of time is

$$\lambda_{0_{\rm tot}} = K\left(\sqrt{\epsilon} + \sqrt{1-\epsilon}\right)\,. \tag{8}$$

The probabilities for each proton hitting the barrier, p_1 and p_2, are

$$p_1 = \frac{\lambda_{0_1}}{\lambda_{0_{\rm tot}}} \quad \text{and} \quad p_2 = \frac{\lambda_{0_2}}{\lambda_{0_{\rm tot}}}\,, \tag{9}$$

and the chance for the two protons hitting simultaneously the barrier is $p_{12} = p_1 \times p_2$. Consequently, the frequency of simultaneous assaults to the barrier for both protons is given by $\lambda_0(\epsilon) = \lambda_{0_{\rm tot}} \times p_{12}$, or

$$\lambda_0(\epsilon) = \frac{\sqrt{2}}{2a}\sqrt{\frac{Q_{\rm 2p}}{\mu_{0\rm V}}}\,\frac{\sqrt{\epsilon}\,\sqrt{1-\epsilon}}{\sqrt{\epsilon}+\sqrt{1-\epsilon}}\,. \tag{10}$$

[Note that: for any ϵ, $\lambda_0(\epsilon) < \lambda_{0_1}(\epsilon)$, $\lambda_0(\epsilon) < \lambda_{0_2}(\epsilon)$, and $\lambda_0(0) = \lambda_0(1) = 0$; also, $\lambda_{0_{\rm max}} = \lambda_0(1/2) = (\sqrt{2}/4)K$].

Here, $a = R_{\rm P} - R_{\rm p}$ is the difference between the radius of the parent nucleus, $R_{\rm P}$, and the proton radius, $R_{\rm p}$ (see below); in equation (10), $\mu_{0\rm V}$ is the reduced mass of the 1p disintegrating system, and it is evaluated as

$$\mu_{0\rm V}{}^{-1} = m_{\rm V}{}^{-1} + m_{\rm p}{}^{-1} \tag{11}$$

where $m_{\rm V}$ is the nuclear mass of the virtual, intermediate product nucleus $(Z_{\rm V}, A_{\rm V})$ as calculated by equation (2);

iv) the probabilities for each proton to tunnel the potential barrier are given by

$$P_{\rm p_1} = {\rm e}^{-G_1(\epsilon)}\,, \quad P_{\rm p_2} = {\rm e}^{-G_2(\epsilon)}\,, \tag{12}$$

where the G's are Gamow's factors related to tunneling through the barrier. These are given by the classical WKB-integral approximation

$$G_{\rm i}(\epsilon) = \frac{2}{\hbar}\int_{s_1}^{s_2}\sqrt{2\mu_{\rm V}(s)\,[V(s) - Q_{\rm p_i}]}\,{\rm d}s\,,\ \ {\rm i} = 1, 2 \tag{13}$$

in which s is the separation between the centres of the proton being emitted and the virtual product nucleus; $V(s)$ is the potential barrier; $\mu_{\rm V}(s)$ is the reduced mass of the 1p disintegrating system; s_1 and s_2 are the inner and outer turning points, respectively; $Q_{\rm p_i}$ is the available energy for the one-proton emission process (see equation (6)); and $\hbar = h/2\pi$ is Planck's constant;

v) the potential barrier creates two adjacent barrier regions, namely, an overlapping and a separation ones; Gamow's factor should, therefore, be calculated over these two barrier regions to obtain $G_{\rm i} = G_{\rm O_i} + G_{\rm S_i}\,({\rm i} = 1, 2)$; $G_{\rm O}$ is calculated over the overlapping region where the proton to be emitted "drives" away from the position $s_1 = a$ until the configuration of contact $s_2 = c = R_{\rm V} + R_{\rm p}$ is reached (here, $R_{\rm V}$ denotes the radius of the virtual, daughter nucleus); on the other hand, $G_{\rm S}$ is calculated through the external, separation barrier region which extends from $s_1 = c$ up to the separation distance $s_2 = b_{\rm i}$, where $V(b_{\rm i}) = Q_{\rm p_i}\,({\rm i} = 1, 2)$ (see figure 2);

vi) as discussed in our previous papers [40, 45, 46], in the overlapping region $(a \leq s \leq c)$ both the quantities $\mu_{\rm V}(s)$ and $V(s)$ have been assumed to follow power functions of exponents $p \geq 0$ and $q \geq 1$, respectively, where the total potential energy at contact configuration (Coulomb-plus-centrifugal potential) is given by

$$V_{\rm c}(c) = \frac{Z_{\rm V}e^2}{c} + \frac{\ell(\ell+1)\hbar^2}{2\mu_{0\rm V}c^2}\,. \tag{14}$$

Here, ℓ is the mutual orbital angular momentum associated with the centrifugal contribution to the barrier, and $e^2 = 1.43996444$ MeV·fm is the elementary electron charge squared; in the separation region ($c \leq s \leq b_{\rm i}$), in turn, the potential energy decreases from $V_{\rm c}(c)$ down to $Q_{\rm p_i}$ (i = 1, 2) following the Coulomb-plus-centrifugal potential energy of the form shown by equation (14) (see figure 2).

By using equation (13) and assumptions *v*) and *vi*) above, Gamow's factors in the overlapping and separation barrier regions have been deduced to give (i = 1, 2)

$$G_{\rm Oi} = \frac{\sqrt{8\mu_{0\rm V}Q_{\rm p_i}}}{\hbar}(c-a)gH_{\rm i}(x_{\rm i},y_{\rm i}) \tag{15}$$

$$G_{\rm Si} = \sqrt{\frac{8\mu_{0\rm V}}{Q_{\rm p_i}}}\frac{e^2}{\hbar}Z_{\rm V}F_{\rm i}(x_{\rm i},y_{\rm i})\,, \tag{16}$$

where the functions H and F read

$$H_{\rm i}(x_{\rm i},y_{\rm i}) = \sqrt{x_{\rm i}+2y_{\rm i}-1} \tag{17}$$

$$F_{\rm i}(x_{\rm i},y_{\rm i}) = \frac{\sqrt{x_{\rm i}}}{2y_{\rm i}}\ln\frac{\sqrt{x_{\rm i}}H_{\rm i}(x_{\rm i},y_{\rm i})+x_{\rm i}+y_{\rm i}}{\sqrt{x_{\rm i}+y_{\rm i}^2}} + \arccos\left[\frac{1}{2}\left(1-\frac{y_{\rm i}-1}{\sqrt{x_{\rm i}+y_{\rm i}^2}}\right)\right]^{1/2} - \frac{H_{\rm i}(x_{\rm i},y_{\rm i})}{2y_{\rm i}}\,, \tag{18}$$

in which $x_{\rm i}$ and $y_{\rm i}$ are given by

$$x_{\rm i} = \frac{\ell(\ell+1)\hbar^2}{\mu_{0\rm V}c^2Q_{\rm p_i}}\,, \quad y_{\rm i} = \frac{1}{2}\frac{Z_{\rm V}e^2}{cQ_{\rm p_i}}\,, \quad i = 1,2\,. \tag{19}$$

The semiempirical character of the present half-life calculation method results from the appearing of a unique parameter, g (see equation (15)). It comes as a combination of the exponents p and q mentioned above in such a way that [40]

$$g = \left(1+\frac{p+q}{2}\right)^{-1}\,, \quad 0 < g \leq 2/3\,. \tag{20}$$

Parameter g is related to the strength of the proton preformation probability through the quantity $\mathrm{e}^{-G_{\rm O}}$. The semiempirical g-value depends upon the source of nuclear data input (mass, radius, half-life) and the values of the physical constants that enter into the routine calculation. For radioactive decays by one-proton emission from non-deformed parent nucleus our previous studies have pointed to $g \approx 0$, thus being indicative of a proton preformation probability very close to unit [44]. However, for deformed parent nuclei, the 1p-decay half-life data have been shown compatible with a $g \lesssim 0.4$ [44]. Since there are indications in the literature that ^{19}Mg, ^{45}Fe, ^{48}Ni, and ^{54}Zn do not exhibit significant deformation [48] we

have assumed $g \approx 0$ in the virtual 1p-transition for these parent nuclei. For the little known, recently discovered ^{67}Kr 2p-emitter nuclide a g-value had to be found semiempirically.

Now, it is convenient to express lengths in fm, masses in u, energies in MeV, and time in s, with which equations (10), (15), (16), and (19) transform to (i = 1,2)

$$\lambda_0(\epsilon) = k_1 \frac{1}{a} \sqrt{\frac{Q_{2\mathrm{p}}}{\mu_{0\mathrm{V}}}} \cdot \frac{\sqrt{\epsilon}\,\sqrt{1-\epsilon}}{\sqrt{\epsilon}+\sqrt{1-\epsilon}} \tag{21}$$

$$G_{\mathrm{Oi}} = k_2(c-a)g\sqrt{\mu_{0\mathrm{V}} Q_{\mathrm{p_i}}}\, H_{\mathrm{i}}(x_{\mathrm{i}}, y_{\mathrm{i}}) \tag{22}$$

$$G_{\mathrm{Si}} = k_3 Z_{\mathrm{V}} \sqrt{\frac{\mu_{0\mathrm{V}}}{Q_{\mathrm{p_i}}}}\, F_{\mathrm{i}}(x_{\mathrm{i}}, y_{\mathrm{i}}) \tag{23}$$

$$x_{\mathrm{i}} = k_4 \frac{\ell(\ell+1)}{\mu_{0\mathrm{V}} c^2 Q_{\mathrm{p_i}}}\,, \quad y_{\mathrm{i}} = k_5 \frac{Z_{\mathrm{V}}}{c Q_{\mathrm{p_i}}}\,, \tag{24}$$

with the constants

$$k_1 = 6.946 \times 10^{21}\,; \quad k_2 = 0.4374703 \text{ s/u}\cdot\text{fm}^2\,; \quad k_3 = 0.6299419 \text{ fm/s}$$
$$k_4 = 20.9008 \text{ MeV}\cdot\text{u}\cdot\text{fm}^2\,; \quad k_5 = 0.71998222 \text{ MeV}\cdot\text{fm}\,. \tag{25}$$

3 Routine calculation to partial 2p-decay half-life

From the considerations above, the total decay constant for a pure nuclear two-proton emission is obtained as

$$\lambda_{\mathrm{T}} = \int_0^1 \lambda(\epsilon)\,\mathrm{d}\epsilon \tag{26}$$

where the decay constant for the mode defined by a given ϵ-value is $\lambda(\epsilon) = \lambda_0(\epsilon)\cdot P(\epsilon)$, in which $\lambda_0(\epsilon)$ is given by (21), and $P(\epsilon)$ represents the probability for simultaneous emission of the two protons, *i.e.*,

$$P(\epsilon) = P_{\mathrm{p_1}} \cdot P_{\mathrm{p_2}} = \exp\left\{-\left[G_1(\epsilon) + G_2(\epsilon)\right]\right\} = \exp\left\{-\left[G_{\mathrm{O1}} + G_{\mathrm{S1}} + G_{\mathrm{O2}} + G_{\mathrm{S2}}\right]\right\}\,. \tag{27}$$

Therefore, using the expressions (21)–(23), $\lambda(\epsilon)$ is obtained as

$$\begin{aligned}\lambda(\epsilon) \;=\; & k_1 \frac{1}{a}\sqrt{\frac{Q_{2\mathrm{p}}}{\mu_{0\mathrm{V}}}} \cdot \frac{\sqrt{\epsilon}\,\sqrt{1-\epsilon}}{\sqrt{\epsilon}+\sqrt{1-\epsilon}} \times \exp\Big\{-k_2(c-a)g\sqrt{\mu_{0\mathrm{V}} Q_{2\mathrm{p}}}\left[\sqrt{\epsilon}\,H_1(x_1,y_1) + \right. \\ & \left. \sqrt{1-\epsilon}\,H_2(x_2,y_2)\right] - k_3 Z_{\mathrm{V}}\sqrt{\frac{\mu_{0\mathrm{V}}}{Q_{2\mathrm{p}}}}\left[\frac{F_1(x_1,y_1)}{\sqrt{\epsilon}} + \frac{F_2(x_2,y_2)}{\sqrt{1-\epsilon}}\right]\Big\}\,,\end{aligned} \tag{28}$$

with

$$x_1 = k_4 \frac{\ell(\ell+1)}{\mu_{0\mathrm{V}} c^2 Q_{2\mathrm{p}}} \cdot \frac{1}{\epsilon}\,; \quad x_2 = \frac{x_1}{\epsilon^{-1}-1}\,; \quad y_1 = k_5 \frac{Z_{\mathrm{V}}}{cQ_{2\mathrm{p}}} \cdot \frac{1}{\epsilon}\,; \quad y_2 = \frac{y_1}{\epsilon^{-1}-1}\,. \tag{29}$$

For a given two-proton radioactive parent nucleus, it is convenient to introduce the new constants as follows:

$$\alpha = k_1 \frac{1}{a}\sqrt{\frac{Q_{2\mathrm{p}}}{\mu_{0\mathrm{V}}}}\,; \quad \beta = k_2(c-a)g\sqrt{\mu_{0\mathrm{V}} Q_{2\mathrm{p}}}\,; \quad \gamma = k_3 Z_{\mathrm{V}}\sqrt{\frac{\mu_{0\mathrm{V}}}{Q_{2\mathrm{p}}}}\,; \tag{30}$$

$$u = \frac{k_4 \ell(\ell+1)}{\mu_{0\mathrm{V}} c^2 Q_{2\mathrm{p}}}\,; \quad v = k_5 \frac{Z_{\mathrm{V}}}{cQ_{2\mathrm{p}}}\,. \tag{31}$$

In this way, equations (28) and (29) are rewritten as

$$\lambda(\epsilon) = \alpha \cdot \frac{\sqrt{\epsilon}\,\sqrt{1-\epsilon}}{\sqrt{\epsilon}+\sqrt{1-\epsilon}} \times \exp\left\{-\beta\left[\sqrt{\epsilon}\,H_1 + \sqrt{1-\epsilon}\,H_2\right] - \gamma\left[\frac{F_1}{\sqrt{\epsilon}} + \frac{F_2}{\sqrt{1-\epsilon}}\right]\right\} \tag{32}$$

and

$$x_1 = \frac{u}{\epsilon}\,; \quad x_2 = \frac{u}{1-\epsilon}\,; \quad y_1 = \frac{v}{\epsilon}\,; \quad y_2 = \frac{v}{1-\epsilon}\,. \tag{33}$$

Finally, once (32) and (33) are inserted into (26), the calculated half-life $T_{1/2} = (\ln 2)/\lambda_{\mathrm{T}}$, or $\tau_{\mathrm{c}} = \log T_{1/2}$, is obtained as

$$\tau_{\mathrm{c}} = -22 + \log\left(a\sqrt{\frac{\mu_{0\mathrm{V}}}{Q_{2\mathrm{p}}}}\right) - \log\int_0^1 J(\epsilon)\,\mathrm{d}\epsilon\,. \tag{34}$$

All that is necessary to evaluate $T_{1/2}$ or τ_{c} is to calculate the integral term $\int_0^1 J(\epsilon)\,\mathrm{d}\epsilon$. For a given 2p-decay case, the quantity $J(\epsilon)$ depends solely upon variable ϵ, and it can be put in the form

$$\begin{aligned} J(\epsilon) \;=\; & \frac{\sqrt{\epsilon}\,\sqrt{1-\epsilon}}{\sqrt{\epsilon}+\sqrt{1-\epsilon}} \times \exp\left\{-\beta\left[w(\epsilon)+z(\epsilon)\right] - \gamma\left[\frac{\sqrt{u}}{2v}\left(\ln\frac{\sqrt{u}\cdot w(\epsilon)+u+v}{\sqrt{u\epsilon+v^2}} + \right.\right.\right. \\ & + \ln\frac{\sqrt{u}\cdot z(\epsilon)+u+v}{\sqrt{u(1-\epsilon)+v^2}}\Bigg) + \frac{1}{\sqrt{\epsilon}}\arccos\left(\frac{1}{2}\left(1-\frac{v-\epsilon}{\sqrt{u\epsilon+v^2}}\right)\right)^{1/2} + \\ & \left.\left.\left. + \frac{1}{\sqrt{1-\epsilon}}\arccos\left(\frac{1}{2}\left(1-\frac{v-(1-\epsilon)}{\sqrt{u(1-\epsilon)+v^2}}\right)\right)^{1/2} - \frac{1}{2v}\left(w(\epsilon)+z(\epsilon)\right)\right]\right\}\,, \end{aligned} \tag{35}$$

where

$$w(\epsilon) = \sqrt{u+2v-\epsilon}\,, \quad z(\epsilon) = \sqrt{u+2v-(1-\epsilon)}\,. \tag{36}$$

$J(\epsilon)$ appears as a bell-shaped curve with maximum at $\epsilon = 1/2$ (see figure 4).

3.1 Other input nuclear quantities of the calculation model

The values of angular momentum, ℓ, associated with the virtual transition $(Z_{\rm P}, A_{\rm P}) \rightarrow (Z_{\rm V} = Z_{\rm P} - 1, A_{\rm V} = A_{\rm P} - 1)$ to be used in the definition of u in (29) have been deduced from the current spin and parity (J^{π}) conservation laws, where the J^{π}-assignments were taken from the most recent evaluation of nuclear properties by Audi *et al.* [29]. This procedure has been used in all half-life estimates (measured and yet unmeasured 2p-decay cases), except for ^{48}Ni and ^{67}Kr parent nuclei, for which cases ℓ has been treated as an adjustable parameter to better reproduce the measured half-life value.

Since the nuclei under investigation are all located near the proton drip line, they are characterized by an abnormal, significant proton-excess, *i.e.*, $2Z/A > 1$. Thus, we have adopted in the present calculation model the evaluation of the average equivalent rms radius of the proton density distribution for both the parent ($R_{\rm P}$) and daughter ($R_{\rm V}$) nuclei following the finite-range droplet model description of atomic nuclei in its spherical approximation as reported by Möller *et al.* [48]. Accordingly, the general expression used here to evaluate the radius-values reads

$$R = r\left[1 + \frac{5}{2}\left(\frac{d}{r}\right)^2\right], \quad r = r_0(1+\bar{\epsilon})\left[1 - \frac{2}{3}\left(1 - \frac{Z}{A}\right)\left(1 - \frac{2Z}{A} - \bar{\delta}\right)\right]A^{1/3}, \tag{37}$$

where $d = 1$ fm is the diffuseness of the nuclear surface, $r_0 = 1.16$ fm, and r represents the nuclear equivalent sharp radius of the proton density distribution. The quantities $\bar{\epsilon}$ and $\bar{\delta}$ in (37) are given by

$$\bar{\epsilon} = 0.25\,{\rm e}^{-0.831A^{1/3}} - 0.191\,A^{-1/3} + 0.0031\,Z^2A^{-4/3} \tag{38}$$

$$\bar{\delta} = \left(1 - \frac{2Z}{A} + 0.004781\frac{Z}{A^{2/3}}\right) \div \left(1 + \frac{2.52114}{A^{1/3}}\right). \tag{39}$$

We recall here that the above radius parametrization does not apply to lighter nuclei of $Z < 8$ and $A < 16$ [48]. Figure 3 shows the variation of the reduced radius of the equivalent liquid-drop model, $R/A^{1/3}$, for nuclei of interest to the present study. The trend reveals a significant decreasing in $R/A^{1/3}$ ($\sim 13\%$) when one passes from ^{19}Mg to ^{67}Kr, thus reflecting a clear degree of nuclear compressibility making, therefore, the simple form $R \propto A^{1/3}$ not valid in estimating radius-values of nuclei of any mass number.

Finally, the value for proton radius used throughout the present calculation model was $R_{\rm p} = 0.87 \pm 0.02$ fm as it comes from the average of proton radius values obtained in different experiments and data analysis on elastic electron scattering from Hydrogen targets [49–53].

In summary, equations (34)–(36) represent a useful tool to estimate 2p-decay half-life of a number of proton-excess nuclides near and beyond the proton drip line. It suffices to know atomic mass-excess values of the participant nuclides from reliable nuclear data sources.

4 Application of the present calculation model to observed 2p-decay cases

So far a few cases, but a number of reliable measurements of 2p-decay half-life, have been reported. Except to lighter 2p-emitter nuclides (^{6}Be, ^{8}C, ^{12}O, and ^{16}Ne), the present calculation method could be applied to other cases of 2p-decay known experimentally up to now (^{19}Mg, ^{45}Fe, ^{48}Ni, ^{54}Zn, and ^{67}Kr parent nuclei; see Table 1).

Figure 4 shows the function $J(\epsilon)$ for $^{19}\mathrm{Mg} \rightarrow {}^{17}\mathrm{Ne} + \mathrm{p} + \mathrm{p}$ and $^{48}\mathrm{Ni} \rightarrow {}^{46}\mathrm{Fe} + \mathrm{p} + \mathrm{p}$ decays with $g = 0$ for both cases and the best ℓ-value for ^{48}Ni as indicated. It is seen that the best chance of occurring simultaneous emission of correlated two protons is when the total available energy, $Q_{2\mathrm{p}}$, is equally shared ($\epsilon = 1/2$) with the virtual one-proton decays.

Figure 5 summarizes the results for the five cases investigated here. The evaluated half-life-values, $\tau_{\mathrm{c}} = \log T_{1/2}(\mathrm{s})$, have been obtained by the routine calculation developed in the precedent sections (see inset table in Fig. 5). τ_{c} results to be a linear function of parameter g. When g increases from 0 to 0.2, for instance, the corresponding half-life increases by $\sim 65\%$ for 2p-decay of ^{19}Mg, and a factor ~ 2 for the other 2p-decay cases here analysed. Such a variation of τ_{c} is within the uncertainties of τ_{c} due to the errors associated with the $Q_{2\mathrm{p}}$-value (a factor ~ 3.5 for ^{19}Mg, ~ 3 for ^{45}Fe and ^{54}Zn, ~ 5 for ^{48}Ni, and ~ 2 for ^{67}Kr).

For ^{19}Mg, ^{45}Fe, and ^{54}Zn 2p-emitter nuclides the same ℓ-assignments as they come from the corresponding J^{π}_{P}- and J^{π}_{V}-values quoted in [29] have led to the calculated half-life values that differ from the measured ones by less than a factor ~ 6 (see Fig. 5).

In the case for ^{48}Ni, in turn, since this nucleus is a doubly-magic parent nucleus (spherical shaped nucleus), according to our previous studies on one-proton radioactivity [44], the best choice was $g = 0$ combined with $\ell = 1$. But, in this case, the spin-parity to be attributed to the product nucleus ^{47}Co from the virtual 1p-emission decay of ^{48}Ni should be $3/2^{-}$ instead of the estimated $7/2^{-}$ as quoted in [29]. On the other hand, for ^{67}Kr parent nucleus the smaller difference between calculated and measured half-life-values ($\sim$ one order of magnitude) was found by using the pair

$\ell = 0$ and $g = 0$. Since in this case the $J^{\pi}_{\rm P}$- and $J^{\pi}_{\rm V}$-assignments are very uncertain nothing can be said at the moment about the $\ell = 0$ found from the present analysis.

To conclude the discussion, it is worthy some words about the simultaneous two-proton preformation probability for the cases under study. This is given by the quantity $P_{\rm 2p} = {\rm e}^{-(G_{\rm O1}+G_{\rm O2})}$, and it represents the probability of finding both protons at the nuclear surface (also known as spectroscopic factor). $P_{\rm 2p}$ is the quantity which measures the simultaneous "arrival" of the two protons at the contact configuration with the virtual ($Z_{\rm V} = Z_{\rm P} - 1, A_{\rm V} = A_{\rm P} - 1$) product nucleus. $G_{\rm O}$ has been introduced in assumption *v*) of sub-section 2.2, and the sum $G_{\rm O1} + G_{\rm O2}$ can be evaluated by using the first term of the exponential factor in equation (28). For a given 2p-decay case $P_{\rm 2p}$ depends upon ℓ, g, and how the total energy available in the 2p-decay is shared between each virtual 1p-decay (the variable $0 \leq \epsilon \leq 1$). When $g = 0$, $P_{\rm 2p} = 1$, which can be interpreted as being both protons "ready" to tunnel the external potential barrier, thus escaping simultaneously outside the atom. This happens in the cases for the quasi spherical ^{19}Mg and spherical ^{45}Fe and ^{48}Ni parent nuclei.

On the other hand, since there are indications of some deformation for both ^{54}Zn and ^{67}Kr parent nuclei [48] the g-values to be used in estimating two-proton preformation probability should be in the interval 0–0.38, and, therefore, $P_{\rm 2p} < 1$. In our previous analysis of one-proton radioactivity [44] the most deformed proton-emitter nuclides were ^{130,131}Eu isotopes, which exhibit a degree of deformation $\delta = 0.28$. By making the correspondence $g = 0.38$ when $\delta = 0.28$, and using the δ-values 0.16 for ^{54}Zn and 0.20 for ^{67}Kr [48] one obtains by linear interpolation $g = 0.215$ for ^{54}Zn and $g = 0.270$ for ^{67}Kr. In these cases the $P_{\rm 2p}$-values are obtained by calculating $P_{\rm 2p} = {\rm e}^{-(G_{\rm O1}+G_{\rm O2})}$ from

$$G_{\rm O1} + G_{\rm O2} = k_2(c-a)g\sqrt{\mu_{0\rm V}Q_{\rm 2p}}\left[\sqrt{u+2v-\epsilon} + \sqrt{u+2v-(1-\epsilon)}\right] . \qquad (40)$$

Calculations have indicated that $P_{\rm 2p}$ does not vary (within 0.1 %) with $0 \leq \epsilon \leq 1$, giving 0.410 and 0.332 for ^{54}Zn and ^{67}Kr, respectively, thus providing evidence for the idea that simultaneous 2p-emission from nuclei is essentially determined by the two-proton penetrability factor ${\rm e}^{-(G_{\rm S1}+G_{\rm S2})}$ through the external, separation barrier region.

5 Half-life predictions for other 2p-decay cases

In Table III of the most recent atomic mass evaluation (the AME2016) by Wang *et al.* [28] one finds about seventy cases of two-proton emitter candidate nuclides located near the proton drip

line. Of these, the more numerous groups are forty-five nuclei in the mass range $3 \leq A \leq 64$ ($3 \leq Z \leq 34$), and fifteen of larger mass number in the range $157 \leq A \leq 186$ ($74 \leq Z \leq 84$). We have selected from the first group of nuclei the small number of 2p-decay cases (fifteen cases) for which $Q_{2p} > 1$ MeV to estimate their partial 2p-decay half-life by applying the present calculation model. Results can be seen in Table 2, where the fifth and sixth columns show the estimated half-lives, $\tau_c = \log T_{1/2}(s)$, found in the range $-15 < \tau_c < -5$ if uncertainties in τ_c are to be considered (nuclei of the second group, although they exhibit $Q_{2p} > 0$, disintegrate promptly by alpha-particle emission). Results show that probably the least difficult cases of 2p radioactivity to be observed are for ^{59}Ge, ^{57}Ga, ^{61}As, and ^{34}Ca nuclides.

As before, ℓ-assignments (column 3) have been obtained from the estimated J^{π}_{P}- and J^{π}_{V}-values as they are quoted in the 2016 evaluation of nuclear properties [29]. Regarding the value of parameter g of the model, it suffices to use $g = 0$ for such a value leads to estimated half-lives that are within the uncertainties coming from errors associated with Q_{2p}-values (see column 6 in Table 2).

On closer inspection, equations (34) and (35), together with parameter γ defined in (30), say us that $\rho = Z_V(\mu_{0V}/Q_{2p})^{1/2}$ is the chief quantity which governs the trend of τ_c, so that we decided to construct figure 6 to get an insight into the 2p-decay process. The data have been grouped according to ℓ-values, and the lighter 2p-emitter nuclides with two-body resonance decay have been also included in figure 6. The trend shows a clear, strong increase of τ_c with the increasing of ρ. Nineteen orders of magnitude of τ_c are displayed for the mass interval $6 \leq A \leq 67$ of the parent nucleus. For the heaviest nuclei of $157 \leq A \leq 186$ ($75 \leq Z \leq 84$) the mass tables indicate $0 < Q_{2p} \lesssim 1.4$ MeV, so that ρ becomes much larger and, therefore, τ_c is expected to increase more strongly, which makes the 2p-decay impossible of being observed, even because of other competitive disintegration processes these nuclei exhibit, mainly the α-decay process. To conclude, Table 2 and figure 6 can be considered as useful tools to help experimental research groups in choosing for new, yet unmeasured cases of 2p radioactivity to be investigated in a future.

6 Final remarks and conclusion

The radioactive decay by the emission of two protons has been experimentally investigated in light and intermediate-mass, proton-rich nuclei during the last six decades or so (Table 1). This is a rare nuclear decay process, very difficult to be detected in view of the extremely low half-lives that have been measured (order of 10^{-21} s for lighter nuclei, picoseconds for the light-massive nucleus

^{19}Mg, and units or tens of milliseconds for intermediate-mass of $44 < A < 68$). Motivated by the recent observation of 2p-decay in ^{67}Kr [27], we decided to develop a simple model based on our previous calculation method applied successfully to 1p-decay, α-decay, and cluster-decay processes to also estimate half-life-values of 2p-decay cases known up to now and new, yet unmeasured cases as well. The 2p-decay process is here treated as a case of simultaneous emission of two protons, but escaping from the nucleus separately (strictly a true 2p-decay). The energy available for this mode of nuclear decay, Q_{2p}, has been estimated from the nuclear (rather than the atomic) mass-values taken from the most recent (AME2016 and NUBASE2016) tabulated values of nuclear properties [28, 29]. The assumption has been made that Q_{2p} is shared between two virtual, intermediate 1p-decay processes of available energies $Q_{p_1} = \epsilon Q_{2p}$ and $Q_{p_2} = (1-\epsilon)Q_{2p}$, $0 \leq \epsilon \leq 1$, thus leading to two intermediate, virtual daughter products ($Z_V = Z - 1, A_V = A - 1$). The decay rate is then obtained by multiplying the probability of each proton to tunnel the complete potential energy barrier (composed of overlapping-plus-centrifugal-plus-Coulomb contributions), by the frequency of simultaneous assaults to the barrier, and summing up all values of ϵ. A closed formula has been derived to calculate the 2p-decay half-life-values which have shown good agreement with the experimental data. The angular momentum-values associated with the virtual 1p-decay resulted compatible with ℓ-values that are deduced from evaluated spin-parity assignment quoted in the most recent tables of nuclear properties [28, 29]. Calculated two-proton preformation probabilities have shown independent of the mode of division of the total energy available in the decay (variable ϵ), so that the decay rate is essentially dictated by the probability of tunneling through the external (Coulomb-plus-centrifugal) barrier. The present study has also shown that partial 2p-decay half-life ($\tau = \log T_{1/2}(\mathrm{s})$) depends strongly upon atomic number of the emitter nuclide, Z, which appears in the definition of the quantity $\rho = (Z-1)(\mu_{0V}/Q_{2p})^{1/2}$ with which τ_c varies by almost twenty orders of magnitude in the range $4 \leq Z \leq 36$. Finally, a few candidate nuclides to 2p-decay have been predicted to have half-lives in the range $-15 \lesssim \tau_c \lesssim -5$, thus with favourable chances of being assessed experimentally.

References

[1] A.H. Becquerel, Sur les radiations invisibles mises par les corps phosphorescent, Compt. Rend. Acad. Sci. (Paris) **122**, 501 (1896).

[2] Y.B. Zeldovich, The existence of new isotopes of light nuclei and the equation of state of neutrons, J. Exptl. Theoret. Phys. (U.S.S.R.) **38**, 1123 (1960) [English translation: JETP

11, 812].

[3] V.I. Goldansky, On neutron-deficient isotopes of light nuclei and the phenomena of proton and two-proton radioactivity, Nucl. Phys. **19**, 482 (1960).

[4] M. Pfützner *et al.*, First evidence for the two-proton decay of ^{45}Fe, Eur. Phys. J. A **14**, 279 (2002).

[5] J. Giovinazzo *et al.*, Two-Proton Radioactivity of ^{45}Fe, Phys. Rev. Lett. **89**, 102501 (2002).

[6] W. Whaling, Magnetic analysis of the Li^6 (He^3, t) Be^6 reaction, Phys. Rev. **150**, 836 (1966).

[7] R.J. Charity *et al.*, Investigations of three-, four-, and five-particle decay channels of levels in light nuclei created using a ^{9}C beam, Phys. Rev. C **84**, 014320 (2011).

[8] G.J. KeKelis, M.S. Zisman, D.K. Scott, R. Jahn, D.J. Vieira, J. Cerny, F. Ajzenberg-Selove, Masses of the unbound nuclei ^{16}Ne, ^{15}F, and ^{12}O, Phys. Rev. C **17**, 1929 (1978).

[9] R.A. Kryger *et al.*, Two-Proton Emission from the Ground State of ^{12}O, Phys. Rev. Lett. **75**, 860 (1995).

[10] D. Suzuki *et al.*, Breakdown of the $Z = 8$ Shell Closure in Unbound ^{12}O and its Mirror Symmetry Phys. Rev. Lett. **103**, 152503 (2009).

[11] C.J. Woodward, R.E. Tribbleand, D.M. Tenner, Mass of ^{16}Ne, Phys. Rev. C **27**, 27 (1983).

[12] P. Voss *et al.*, ^{19}Mg two-proton decay lifetime, Phys. Rev. C **90**, 014301 (2014).

[13] I. Mukha *et al.*, Observation of Two-Proton Radioactivity of ^{19}Mg by Tracking the Decay Products, Phys. Rev. Lett. **99**, 182501 (2007).

[14] I. Mukha *et al.*, Experimental studies of nuclei beyond the proton drip line by tracking technique, Eur. Phys. J. A **42**, 421 (2009).

[15] K. Miernik *et al.*, Two-Proton radioactivity of ^{45}Fe, Eur. Phys. J. A **42**, 431 (2009).

[16] K. Miernik *et al.*, Two-Proton Correlations in the Decay of ^{45}Fe, Phys. Rev. Lett. **99**, 192501 (2007).

[17] L. Audirac *et al.*, Direct and β-delayed multiproton emission from atomic nuclei with a time projection chamber: the cases of ^{43}Cr, ^{45}Fe, and ^{51}Ni, Eur. Phys. J. A **48**, 179 (2012).

[18] J. Giovinazzo *et al.*, First Direct Observation of Two Protons in the Decay of ^{45}Fe with a Time-Projection-Chamber, Phys. Rev. Lett. **99**, 102501 (2007).

[19] J. Giovinazzo *et al.*, Two-proton decay of ^{45}Fe: a new type of radioactivity, Nucl. Phys. A **722**, 434c (2003).

[20] C. Dossat *et al.*, Two-Proton Radioactivity Studies with ^{45}Fe and ^{48}Ni, Phys. Rev. C **72**, 054315 (2005).

[21] J. Giovinazzo, Two-proton radioactivity in the $A \sim 50$ mass region, J. Phys. G: Nucl. Part. Phys. **31**, S1509 (2005).

[22] M. Pomorski *et al.*, First observation of two-proton radioactivity in ^{48}Ni, Phys. Rev. C **83**, 061303(R) (2011).

[23] M. Pomorski *et al.*, Studies of ^{48}Ni Using the Optical Time Projection Chamber, Acta Phys. Pol. B **43**, 267 (2012).

[24] M. Pomorski *et al.*, Proton Spectroscopy of ^{48}Ni, ^{46}Fe, and ^{44}Cr, Phys. Rev. C **90**, 014311 (2014).

[25] B. Blank *et al.*, First Observation of ^{54}Zn and its Decay by Two-Proton Emission, Phys. Rev. Lett. **94**, 232501 (2005).

[26] P. Ascher *et al.*, Direct Observation of Two Protons in the Decay of ^{54}Zn, Phys. Rev. Lett. **107**, 102502 (2011).

[27] T. Goigoux *et al.*, Two-proton radioactivity of ^{67}Kr, Phys. Rev. Lett. **117**, 162501 (2016).

[28] M. Wang, G. Audi, F.G. Kondev, W.J. Huang, S. Naimi, X. Xu, The AME2016 atomic mass evaluation (II) Tables, graphs and references, Chin. Phys. C **41**, 030003 (2017).

[29] G. Audi, F.G. Kondev, M. Wang, W.J. Huang, S. Naimi, The NUBASE2016 evaluation of nuclear properties, Chin. Phys. C **41**, 030001 (2017).

[30] B. Alex Brown, Diproton decay of nuclei on the proton drip line, Phys. Rev. C **43**, R1513 [Erratum: Phys. Rev. C **44**, 924] (1991).

[31] W.E. Ormand, Properties of proton drip-line nuclei at the sd-fp-shell interface, Phys. Rev. C **53**, 214 (1966).

[32] W. Nazarewicz, J. Dobaczewski, T.R. Werner, J.A. Maruhn, P.-G. Reinhard, K. Rutz, C.R. Chinn, A.S. Umar, M.R. Strayer, Structure of proton drip-line nuclei around doubly magic ^{48}Ni, Phys. Rev. C **53**, 740 (1996).

[33] B.J. Cole, Stability of proton-rich nuclei in the upper sd shell and lower pf shell, Phys. Rev. C **54**, 1240 (1996).

[34] L.V. Grigorenko, R.C. Johnson, I.G. Mukha, I.J. Thompson, M.V. Zhukov, Two-proton radioactivity and three-body decay: General problems and theoretical approach, Phys. Rev. C **64**, 054002 (2001).

[35] L.V. Grigorenko, M.V. Zhukov, Two-proton radioactivity and three-body decay II Exploratory studies of lifetimes and correlations, Phys. Rev. C **68**, 054005 (2003).

[36] M. Pfützner, M. Karny, L.V. Grigorenko, K. Riisager, Radioactive decays at limits of nuclear stability, Rev. Mod. Phys. **84**, 567 (2012).

[37] E. Olsen, M. Pfützner, N. Birge, M. Brown, W. Nazarewicz, A. Perhac, Landscape of Two-Proton Radioactivity, Phys. Rev. Lett. **110**, 222501 (2013); Erratum: Phys. Rev. Lett. **111**, 139903 (2013).

[38] D.S. Delion, R.J. Liotta, R. Wyss, Simple approach to two-proton emission, Phys. Rev. C **87**, 034328 (2013).

[39] M. Gonçalves, N. Teruya, O.A.P. Tavares, S.B. Duarte, Two-proton emission half-lives in the effective liquid drop model, Phys. Lett. B **774**, 14 (2017).

[40] O.A.P. Tavares, E.L. Medeiros, M.L. Terranova, Alpha decay half-life of bismuth isotopes, J. Phys. G: Nucl. Part. Phys. **31**, 129 (2005).

[41] O.A.P. Tavares, M.L. Terranova, E.L. Medeiros, New evaluation of alpha decay half-life of ^{190}Pt isotope for the Pt-Os dating system, Nucl. Instrum. Methods Phys. Res. B **243**, 256 (2006).

[42] E.L. Medeiros, M.M.N. Rodrigues, S.B. Duarte, O.A.P. Tavares, Systematics of alpha-decay half-life: new evaluations for alpha-emitter nuclides, J. Phys. G: Nucl. Part. Phys. **32**, B23 (2006).

[43] O.A.P. Tavares, E.L. Medeiros, Natural and artificial alpha radioactivity of Platinum isotopes, Phys. Scr. **84**, 045202 (2011).

[44] O.A.P. Tavares, E.L. Medeiros, Proton radioactivity: the case for ^{53m}Co proton-emitter isomer, Eur. Phys. J. A **45**, 57 (2010).

[45] O.A.P. Tavares, L.A.M. Roberto, E.L. Medeiros, Radioactive decay by the emission of heavy nuclear fragments, Phys. Scr. **76**, 375 (2007).

[46] O.A.P. Tavares, E.L. Medeiros, A simple description of cluster radioactivity, Phys. Scr. **86**, 015201 (2012).

[47] K-N. Huang, M. Aoyagi, M.H. Chen, B. Crasemann, H. Mark, Neutral-atom electron binding energies from relaxed-orbital relativistic Hartree-Fock-Slater calculations $2 \leq Z \leq 106$, At. Data Nucl. Data Tables **18**, 243 (1976).

[48] P. Möller, J.R. Nix, W.D. Myers, W.J. Swiatecki, Nuclear ground-state masses and deformations, At. Data Nucl. Data Tables **59**, 185 (1995).

[49] P. Mergell, Ulf-G. Meißner, D. Drechsel, Dispersion-theoretical analysis of the nucleon electromagnetic form factors, Nucl. Phys. A **596**, 367 (1996).

[50] G.G. Simon, Ch. Schmitt, F. Borkowski, V.H. Walther, Absolute electron-proton cross sections at low momentum transfer measured with a high pressure gas target sysem, Nucl. Phys. A **333**, 381 (1980).

[51] F. Borkowski, G.G. Simon, V.H. Walther, R.D. Wendling, Electromagnetic form factors of the proton at low four-momentum transfer (II), Nucl. Phys. B **93**, 461 (1975).

[52] I. Sick, On the rms-radius of the proton, Phys. Lett. B **576**, 62 (2003).

[53] K. Melnikov, T. Ritbergen, Three-loop slope of the Dirac form factor and the $1S$ Lamb shift in hydrogen, Phys. Rev. Lett. **84**, 1673 (2000).

Table 1: Observed cases of two-proton radioactivity known up today.

2p-decay case	Q_{2p} (MeV)[a]	Measured 2p-decay half-life		Reference
		$\tau_e = \log T_{1/2}$ (s)	Uncertainty in τ_e[b]	
^{6}Be $\rightarrow$ ^{4}He	1.372 ± 0.005	-20.30[c]	$[-20.32, -20.26]$	[6]
^{8}C $\rightarrow$ ^{6}Be	2.112 ± 0.019	-20.46[c]	$[-20.60, -20.24]$	[7]
^{12}O $\rightarrow$ ^{10}C	1.639 ± 0.024	-20.94[c]	$[-21.13, -20.53]$	[8]
		-21.10[c]	$[-21.23, -20.92]$	[9]
		-21.15[c]	$[-21.40, -20.34]$	[10]
^{16}Ne $\rightarrow$ ^{14}O	1.402 ± 0.021	-20.64[c]	———	[8]
		-20.38[c]	———	[11]
^{19}Mg $\rightarrow$ ^{17}Ne	0.752 ± 0.050	-11.55	$[-11.59, -11.52]$	[12]
		-11.40	$[-11.60, -11.26]$	[13, 14]
^{45}Fe $\rightarrow$ ^{43}Cr	1.160 ± 0.035	-2.43	$[-2.48, -2.39]$	[15, 16]
		-2.42	$[-2.45, -2.40]$	[17]
		-2.46	$[-2.57, -2.29]$	[18]
		-2.33	$[-2.48, -2.09]$	[5, 19]
		-2.40	$[-2.57, -2.15]$	[4]
		-2.55	$[-2.68, -2.45]$	[20]
		-2.64	$[-2.77, -2.44]$	[21]
^{48}Ni $\rightarrow$ ^{46}Fe	1.312 ± 0.061	-2.52	$[-2.74, -2.28]$	[22–24]
^{54}Zn $\rightarrow$ ^{52}Ni	1.487 ± 0.045	-2.43	$[-2.57, -2.24]$	[21, 25]
		-2.70	$[-2.80, -2.57]$	[26]
^{67}Kr $\rightarrow$ ^{65}Se	1.700 ± 0.017[d]	-1.70	$[-1.92, -1.55]$	[27]

[a] Calculated values by using equation (5) and mass-excess-values taken from the AME2016 by Wang *et al.* [28]; the quoted uncertainties are of the order of the experimental ones.

[b] The reported τ_e-uncertainty interval includes the measured half-life uncertainty when available.

[c] This is calculated from the measured total level width, Γ, of the resonance two-body decay through the equation $\tau_e = -18.34 - \log \Gamma\,(\text{keV})$ (see [29]).

[d] Measured value as reported in [27] plus the screening to the nucleus due to the surrounding electrons [see equation (4)].

Table 2: Predicted values of true 2p-decay half-life for some proton-rich nuclei.

2p-decay case[a]	$Q_{2p} \pm \delta Q_{2p}$ (MeV)[b]	ℓ [c]	$\rho\,(\mathrm{u/MeV})^{1/2}$ [d]	Partial 2p-decay half-life[e]	
				τ_c	uncertainty in τ_c
^{22}Si $\rightarrow$ ^{20}Mg	1.28 ± 0.05	2	11.26 ± 0.22	-9.67	$[-9.95, -9.37]$
^{26}S $\rightarrow$ ^{24}Si	1.76 ± 0.07	0	11.13 ± 0.22	-14.51	$[-14.77, -14.23]$
^{28}Cl $\rightarrow$ ^{26}P	1.97 ± 0.08	2	11.23 ± 0.23	-11.19	$[-11.48, -10.88]$
^{30}Ar $\rightarrow$ ^{28}S	2.28 ± 0.09	0	11.11 ± 0.22	-15.12	$[-15.38, -14.85]$
^{32}K $\rightarrow$ ^{30}Cl	2.08 ± 0.08	2	12.33 ± 0.24	-10.62	$[-10.92, -10.30]$
^{34}Ca $\rightarrow$ ^{32}Ar	1.48 ± 0.06	2	15.44 ± 0.31	-7.03	$[-7.42, -6.62]$
^{36}Sc $\rightarrow$ ^{34}K	2.00 ± 0.08	0	13.99 ± 0.28	-12.47	$[-12.80, -12.12]$
^{38}Ti $\rightarrow$ ^{36}Ca	2.75 ± 0.11	3	12.54 ± 0.25	-8.95	$[-9.28, -8.59]$
^{40}V $\rightarrow$ ^{38}Sc	1.85 ± 0.07	1	16.03 ± 0.30	-9.44	$[-9.81, -9.06]$
^{56}Ga $\rightarrow$ ^{54}Cu	3.45 ± 0.14	1	16.06 ± 0.33	-11.62	$[-12.00, -11.21]$
^{57}Ga $\rightarrow$ ^{55}Cu	2.05 ± 0.08	1	20.84 ± 0.41	-5.80	$[-6.29, -5.29]$
^{58}Ge $\rightarrow$ ^{56}Zn	3.74 ± 0.15	1	15.95 ± 0.32	-12.01	$[-12.38, -11.61]$
^{59}Ge $\rightarrow$ ^{57}Zn	2.11 ± 0.08	1	21.23 ± 0.40	-5.58	$[-6.06, -5.07]$
^{60}As $\rightarrow$ ^{58}Ga	3.50 ± 0.14	1	17.02 ± 0.34	-10.95	$[-11.35, -10.53]$
^{61}As $\rightarrow$ ^{59}Ga	2.29 ± 0.09	1	21.05 ± 0.41	-6.07	$[-6.56, -5.55]$

[a] These are fifteen selected cases of $Q_{2p} > 1.0$ MeV.

[b] Calculated values as described in the text [equation (5)]; an average of $\sim 4\%$ uncertainty to Q_{2p}-value has been assumed following the measured cases in Table 1.

[c] Mutual angular momentum for the virtual transition by 1p emission from the parent nucleus (see text and figure 1).

[d] $\rho = Z_V(\mu_{0V}/Q_{2p})^{1/2}$, the chief quantity of the present model upon which the variation of half-life has been investigated (see figure 6).

[e] $\tau_c = \log T_{1/2}\,(\mathrm{s})$; the uncertainty associated with τ_c-value comes from δQ_{2p}; in all cases τ_c is obtained at $g = 0$.

Figure Captions

Fig. 1 Schematic representation of a true nuclear two-proton decay process. Protons p_1 and p_2 are thought to be emitted separately and simultaneously from a parent nucleus leading to intermediate, virtual daughter products (Z_V, A_V), but to a final daughter nucleus (Z_D, A_D). The total available energy, Q_{2p}, is shared between the two Q-values for the emission of each proton, $Q_{p_1} = \epsilon Q_{2p}$ and $Q_{p_2} = (1-\epsilon)Q_{2p}$, to allow (or not) their simultaneous emission by varying ϵ continuously in the interval $0 \leq \epsilon \leq 1$.

Fig. 2 Potential barrier, $V(s)$, for the virtual one-proton decay processes in two-proton radioactive decay mode of ^{32}K parent nucleus as an illustrative example. The overlapping barrier region $(a \leq s \leq c)$ is emphasized by the shaded area. In the external barrier region $(c \leq s \leq b)$ the total potential barrier (full line) comprises the Coulomb (dotted line) and centrifugal (short-dashed line) contributions. The horizontal large-dashed line indicates the Q_{1p}-value when both protons have the same chance of escaping.

Fig. 3 Reduced radius of the equivalent liquid-drop model $(R/A^{1/3})$ for the average equivalent rms radius of the proton density distribution, R, according to the finite-range nuclear liquid droplet model by Möller *et al.* [48] for the proton-excess nuclei indicated (for details see section 3.1); the full line shows the trend.

Fig. 4 The function $J(\epsilon)$ [equations (35) and (36)] for two cases of 2p radioactivity as indicated. The best chance to occur the emission of two protons simultaneously is at $\epsilon = 0.5$, *i.e.*, when the total available energy is shared equally for the emission of each proton.

Fig. 5 Partial 2p-decay half-life, $\tau = \log T_{1/2}\,(\mathrm{s})$, versus atomic number of the parent nucleus, Z_P, for the known cases of 2p radioactivity. Full symbols indicate experimental data, and open ones calculated results following the present model (Section 3). The lines joining the points are to show the general trend of τ vs Z_P. The inset table shows a comparison between experimental (τ_e) and calculated (τ_c) data. Uncertainties in the values of τ_e and τ_c are of the order of the symbol sizes. Experimental data for lighter 2p-emitter nuclides are also shown, although the present model is not applicable to these cases.

Fig. 6 Partial 2p-decay half-life, $\tau = \log T_{1/2}\,(\mathrm{s})$, plotted against the quantity $\rho = Z_V(\mu_{0V}/Q_{2p})^{1/2}$. Experimental points (weighted average of data in Table 1) are represented by closed circles. Open circles represent estimated τ_c-values for some proton-rich nuclei according to the present calculation model. Part (a) groups the cases of $\ell = 0$, and part (b) those of $\ell = 1$

and $\ell = 2$ (parent nuclei are shown near the data points). Experimental as well as calculated uncertainties are of the order of the symbol sizes.

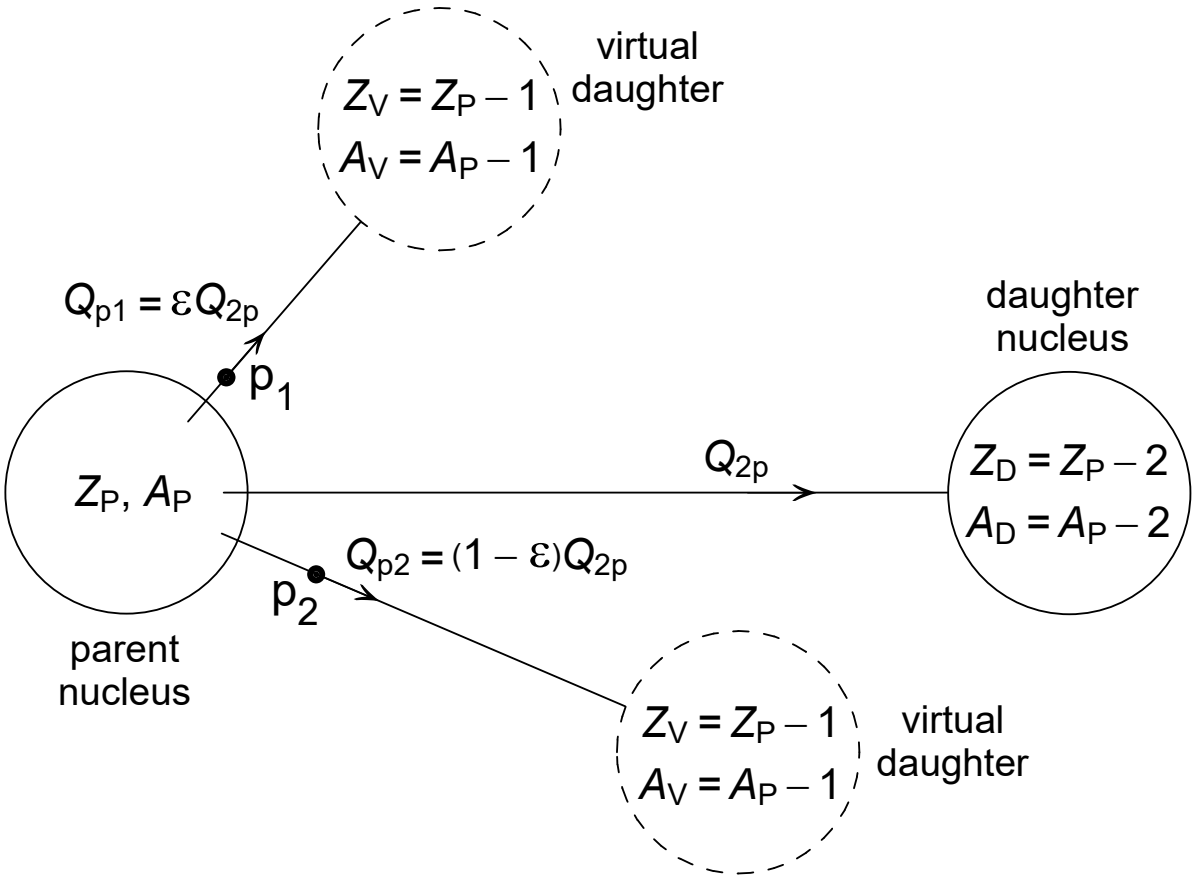
virtual
daughter
$Z_V = Z_P - 1$
$A_V = A_P - 1$
$Q_{p1} = \varepsilon Q_{2p}$
p_1
daughter
nucleus
Q_{2p}
Z_P, A_P
$Z_D = Z_P - 2$
$A_D = A_P - 2$
$Q_{p2} = (1 - \varepsilon) Q_{2p}$
p_2
parent
nucleus
$Z_V = Z_P - 1$
$A_V = A_P - 1$
virtual
daughter

Figure 1:

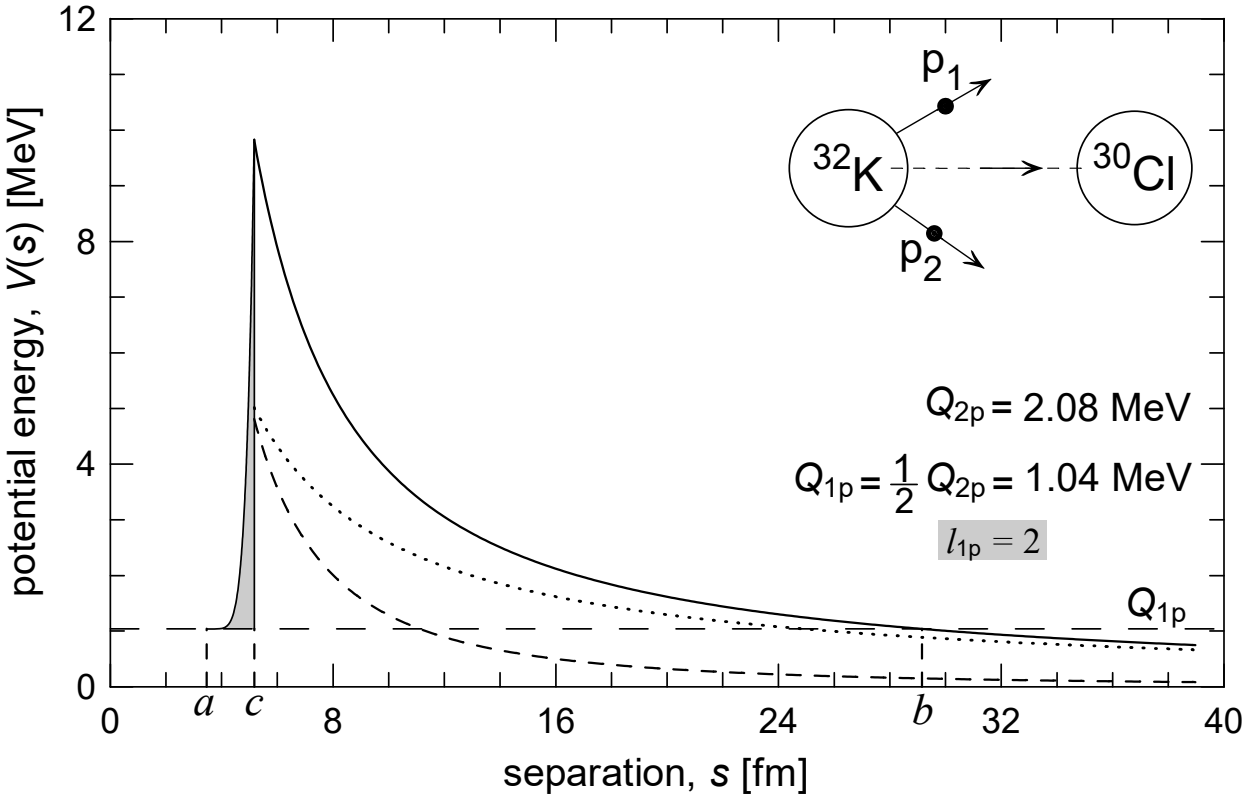
12
8
4
0
potential energy, V(s) [MeV]
0
8
16
24
32
40
separation, s [fm]
a
c
b
p1
p2
32K
30Cl
Q2p = 2.08 MeV
Q1p = 1/2 Q2p = 1.04 MeV
l1p = 2
Q1p

Figure 2:

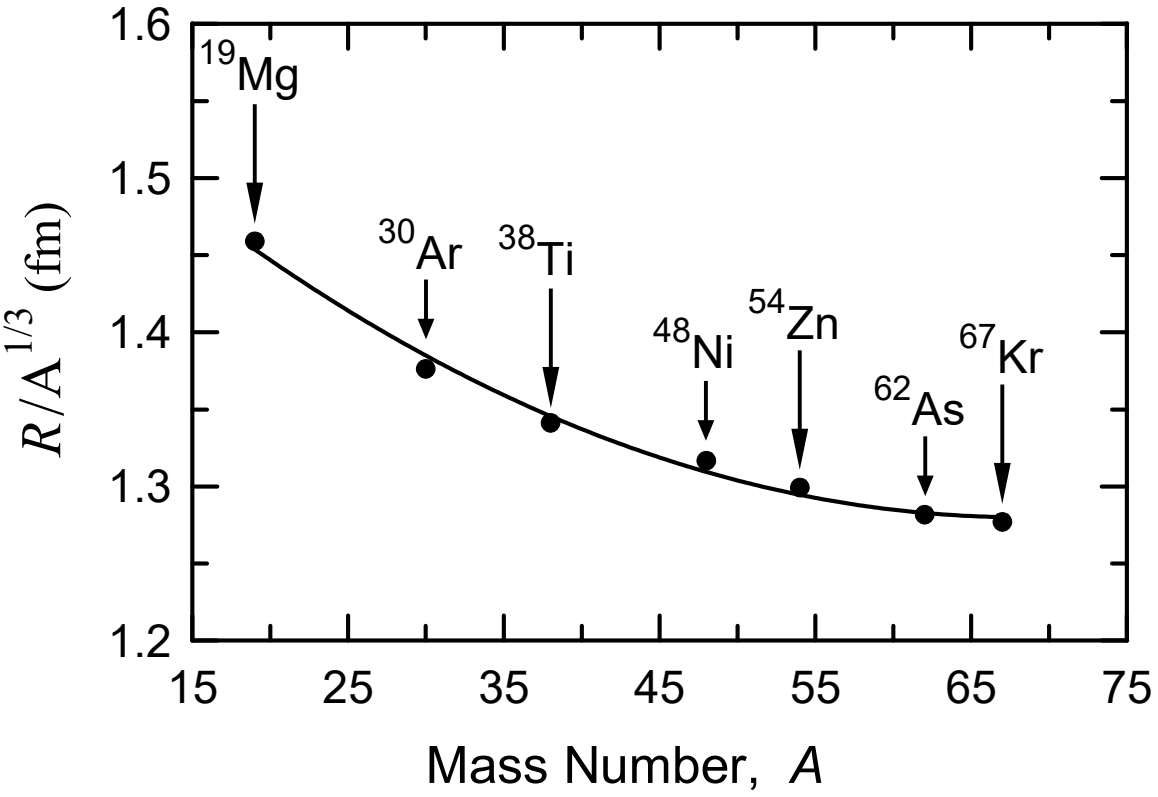
1.6
1.5
1.4
1.3
1.2
15
25
35
45
55
65
75
$R/A^{1/3}$ (fm)
Mass Number, A
^{19}Mg
^{30}Ar
^{38}Ti
^{48}Ni
^{54}Zn
^{62}As
^{67}Kr

Figure 3:

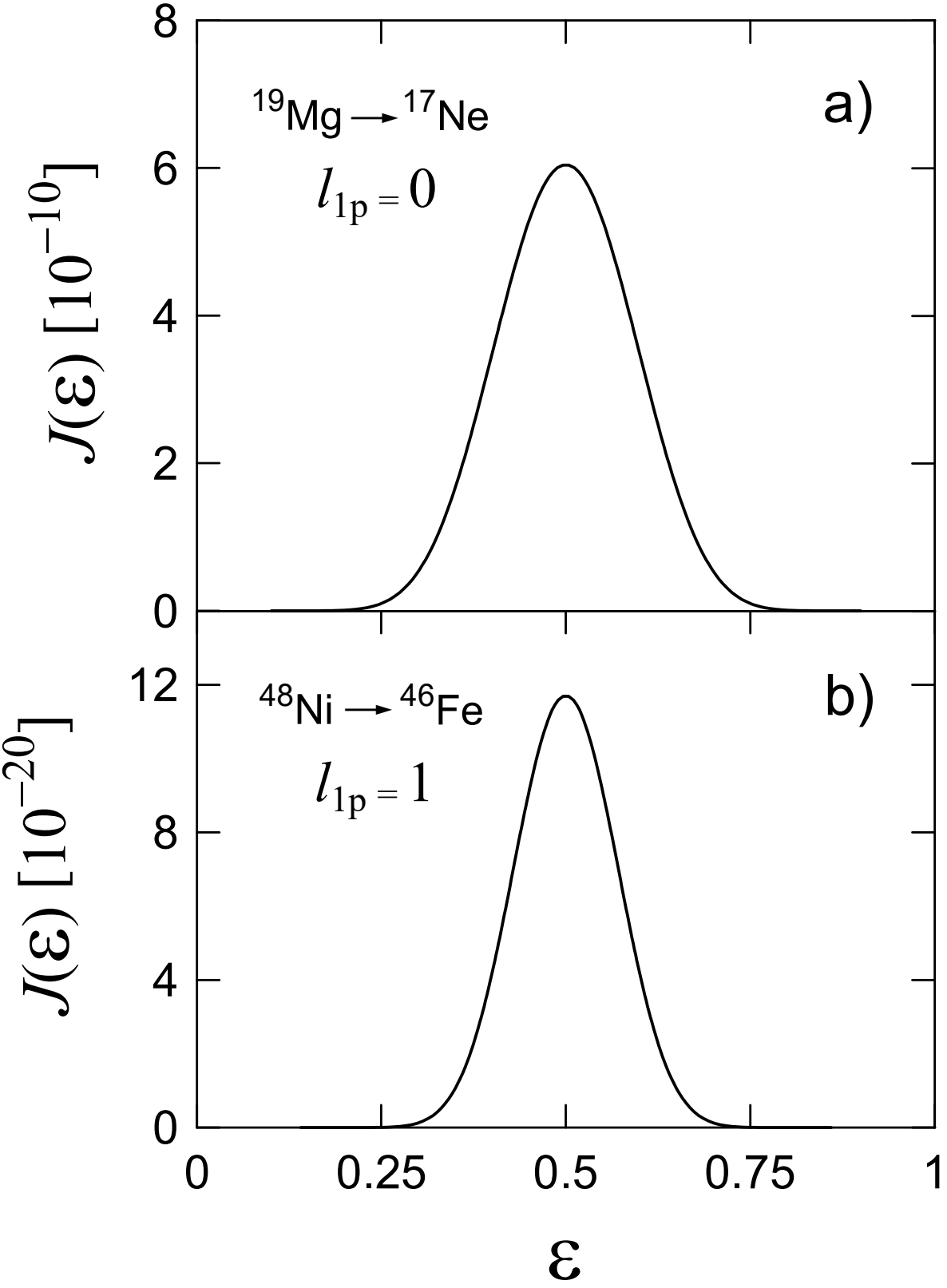
a)
^{19}Mg → ^{17}Ne
$l_{1p} = 0$
$J(\varepsilon)$ [10^{-10}]
b)
^{48}Ni → ^{46}Fe
$l_{1p} = 1$
$J(\varepsilon)$ [10^{-20}]
0
2
4
6
8
12
0.25
0.5
0.75
1
ε

Figure 4:

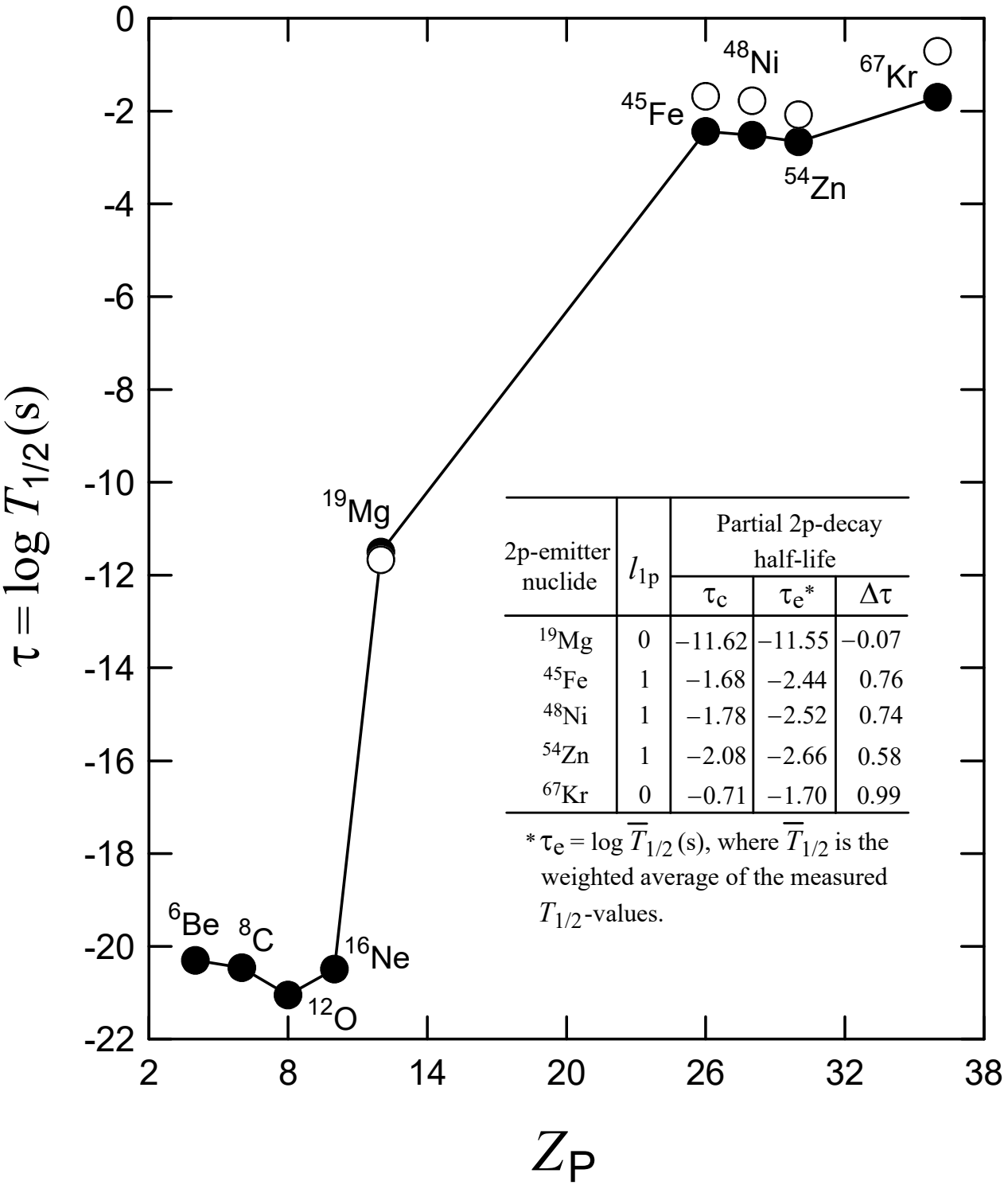

2p-emitter nuclide	l_{1p}	Partial 2p-decay half-life		
		τ_c	τ_e*	$\Delta\tau$
^{19}Mg	0	−11.62	−11.55	−0.07
^{45}Fe	1	−1.68	−2.44	0.76
^{48}Ni	1	−1.78	−2.52	0.74
^{54}Zn	1	−2.08	−2.66	0.58
^{67}Kr	0	−0.71	−1.70	0.99

* $\tau_e = \log \overline{T}_{1/2}$ (s), where $\overline{T}_{1/2}$ is the weighted average of the measured $T_{1/2}$-values.

Figure 5:

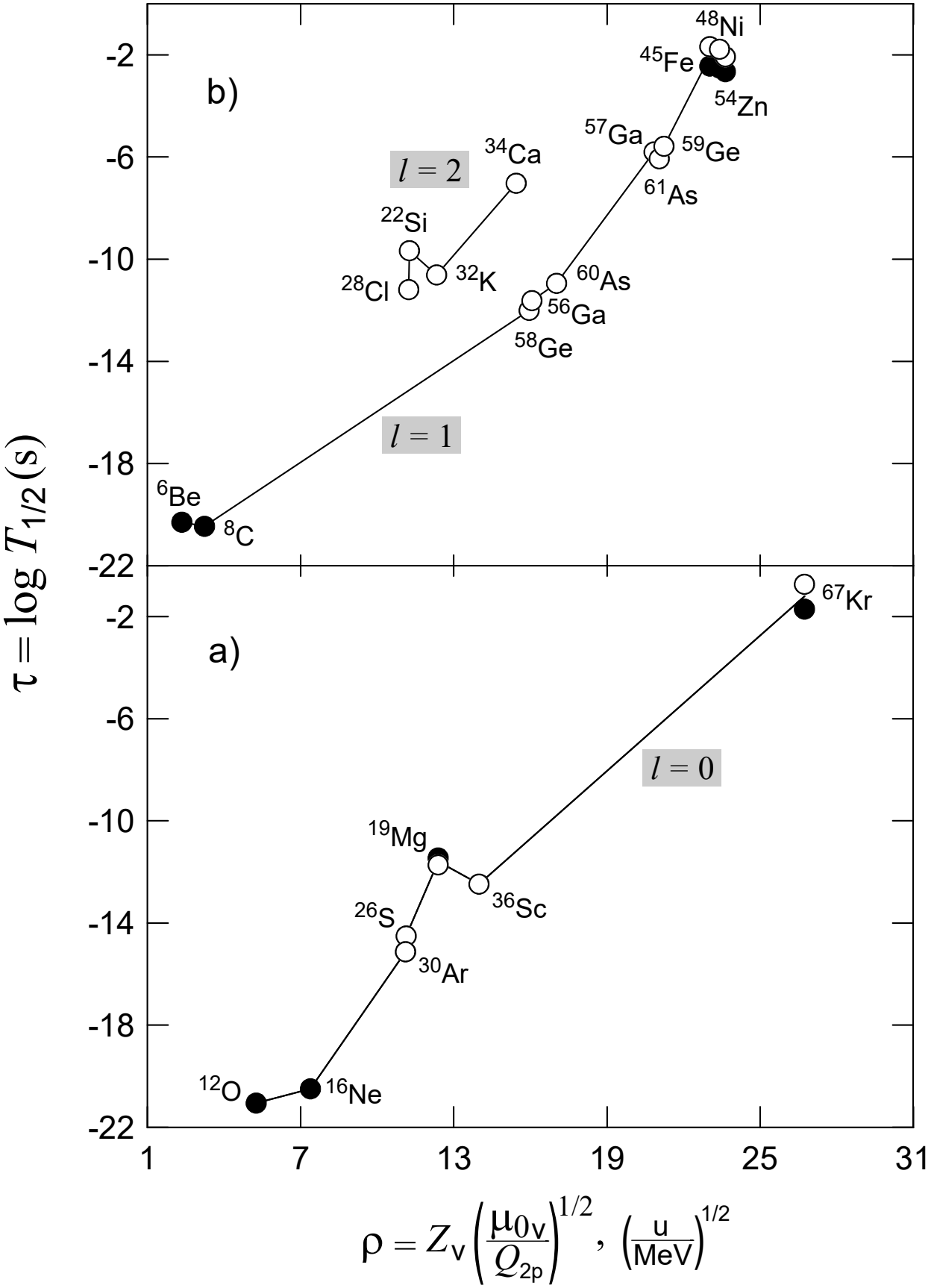
b)
a)
$l = 2$
$l = 1$
$l = 0$
^{48}Ni
^{45}Fe
^{54}Zn
^{57}Ga
^{59}Ge
^{61}As
^{34}Ca
^{22}Si
^{28}Cl
^{32}K
^{60}As
^{56}Ga
^{58}Ge
^{6}Be
^{8}C
^{67}Kr
^{19}Mg
^{36}Sc
^{26}S
^{30}Ar
^{12}O
^{16}Ne
-2
-6
-10
-14
-18
-22
1
7
13
19
25
31
$\tau = \log T_{1/2}(\mathrm{s})$
$\rho = Z_{\nu}\left(\frac{\mu_{0\nu}}{Q_{2p}}\right)^{1/2}, \left(\frac{\mathrm{u}}{\mathrm{MeV}}\right)^{1/2}$

Figure 6:

NOTAS DE FÍSICA é uma pré-publicação de trabalho original em Física.
Pedidos de cópias desta publicação devem ser enviados aos autores ou ao:

Centro Brasileiro de Pesquisas Físicas
Área de Publicações
Rua Dr. Xavier Sigaud, 150 – 4º andar
22290-180 – Rio de Janeiro, RJ
Brasil
E-mail: socorro@cbpf.br/valeria@cbpf.br
http://portal.cbpf.br/publicacoes-do-cbpf

NOTAS DE FÍSICA is a preprint of original unpublished works in Physics.
Requests for copies of these reports should be addressed to:

Centro Brasileiro de Pesquisas Físicas
Área de Publicações
Rua Dr. Xavier Sigaud, 150 – 4º andar
22290-180 – Rio de Janeiro, RJ
Brazil
E-mail: socorro@cbpf.br/valeria@cbpf.br
http://portal.cbpf.br/publicacoes-do-cbpf